Estimation of the Radiated Emission from a Protective Turn of a Meander Line in the Air

Adnan Alhaj Hasan
Scientific Research Laboratory of Basic Research
on Electromagnetic Compatibility
Tomsk State University of Control Systems and Radioelectronics
Tomsk, Russia
alhaj.hasan.adnan@yandex.ru

Talgat R. Gazizov
Scientific Research Laboratory of Basic Research
on Electromagnetic Compatibility
Tomsk State University of Control Systems and Radioelectronics
Tomsk, Russia
talgat@tu.tusur.ru

***Abstract*—This paper investigates an algorithm for estimating the radiated emission from transmission lines using quasi-static analysis. The algorithm was tested on a meander line turn of two coupled wires above the ground plane in the air dielectric filling. The dependences of the cross-section parameters and the characteristics of the turn on the temperature at the frequency of 10 GHz were obtained. Examples of the radiation patterns at different frequencies, as well as the current distributions are given. Frequency dependences of the maximum values of the electric field strength obtained by two approaches: quasi-static and electrodynamic are compared. The results were obtained and compared for the meander line with optimal parameters and for the unmatched meander line and compared with the results of a single matched transmission line of one wire over the ground plane and an unmatched one. It is noted that the results of quasi-static and electrodynamic analyses are close at low frequencies but the difference increases at high ones. It was revealed that the meander line structures are able to minimize the radiated emission in the most frequency range except at the resonance frequencies. The tested algorithm gave acceptable results comparing to electrodynamic analysis.**

Keywords— meander line, radiated emission, quasi-static, electrodynamic, temperature

I. Introduction

The application field of meander lines (ML) in radio-electronic devices (RED) is quite wide, for example the superconductive microwave meander lines as in [1], or using the antenna meander line for maximum efficiency and minimal environmental impact as in [2] and to suppress spurious emissions as in [3]. Previously, their properties have been studied, for example in [4]. The use of MLs for signal filtering in the frequency band [5, 6] and for protection against an ultrashort pulse [7] has been investigated. However, MLs have been poorly inquired in terms of radiated emissions which can affect the operation of REDs, but the interest exists like in the important work of [8]. In particular, MLs have not been examined in the temperature range. This may be due to the computational cost of electrodynamic analysis. Meanwhile, in [9], an algorithm based on quasi-static analysis which requires less computational costs is proposed to estimate the radiated emissions. The purpose of this work is to perform a comparative evaluation of the radiated emission from a protective ML turn of two coupled wires above the ground plane in an air dielectric filling, and to investigate the effect of temperature on the characteristics of the ML.

II. Initial Data

A simple structure of the ML turn based on two coupled wires above the ground plane in an air dielectric filling was modeled. The simulation was carried out without taking into account losses in the wires. The geometric model of the ML cross-section constructed in the TALGAT system is shown in Fig. 1, where the distance between the wires S=14.71 μm, the distance from the ground layer to the signal wire H=5.05 mm, and the wire radius R=50 μm. The circuit model is shown in Fig. 2. The ML consists of two parallel wires with a length of l=30 mm connected to each other at the far end. One of the wires at the near end is connected to a source of pulse signal represented in the circuit by an ideal EMF source (firstly to calculate the frequency response in the form of a trapezoid of 1 V and the rise and fall times of 50 ps, and a flat top of 100 ps, and then, to calculate currents and electric field strength in the far zone, in the form of a sinusoid with an EMF amplitude of 1 V) and internal resistance $R1$. The other wire is connected to the receiving device represented in the circuit by the resistance $R2$. The number of segments on each wire (n) is 640. The matrix of per-unit-length coefficients of electrostatic induction is taken to be equal to

$$\mathbf{C} = \begin{bmatrix} 54.791 & -49.007 \\ -49.007 & 54.791 \end{bmatrix} \text{pF/m}. \quad (1)$$

The matrix was calculated at the length of 0.5 μm for the subintervals at the wires cross-section boundaries.

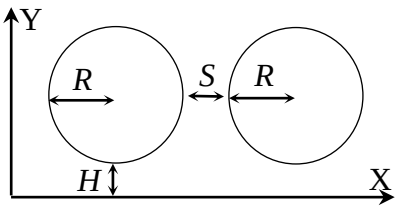

Fig. 1. The geometric model of the ML cross-section.

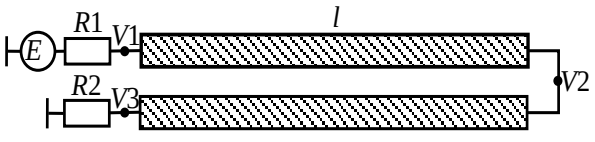

Fig. 2. The ML circuit model.

To minimize the reflection at the ends of the wires, the values of $R1$ and $R2$ are chosen to be equal to the geometric mean of the wave resistances of the even (Z_e) and odd (Z_o) modes of the line.

The work was carried out with the financial support of the Ministry of Science and Higher Education of the Russian Federation (Project FEWM-2020-0041) in TUSUR.

III. SIMULATION RESULTS FOR THE ML WITH OPTIMAL PARAMETERS

The values of the ML parameters are assumed to be optimal if they satisfy the criterion of equality of the amplitudes of the first two pulses at the ML output in the time response to the trapezoidal pulse excitation (Fig. 3). As can be seen from Fig. 3, the amplitudes of the first two pulses are equal. Using the algorithm from [9] (quasi-static analysis), we calculated the current distributions and obtained the radiation pattern (RP). Current distributions in the ML at the frequencies of 0.5, 5 and 10 GHz are shown in Fig. 4. Moreover, Fig. 5 shows an example of an RP at the frequency of 0.5 GHz and a distance of 1 m, with a change of φ and θ from 0° to 180° with a step of 1°.

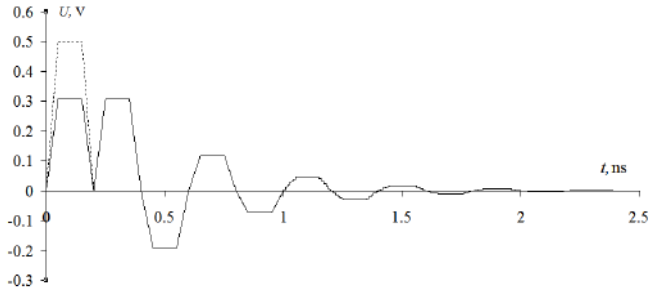

Fig. 3. The voltage waveforms at the beginning (- -) and end of the ML (——).

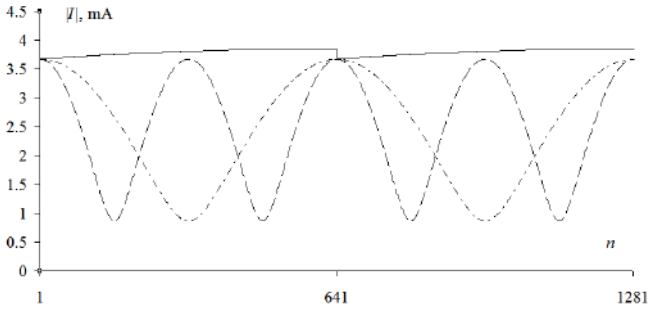

Fig. 4. The current distributions in the ML at frequencies of 0.5 (–) and 5 (- – -) and 10 GHz (– –).

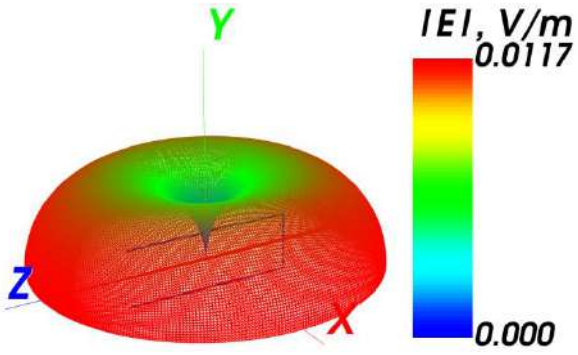

Fig. 5. An example of an RP for the ML built in TALGAT.

The same structure was modeled in the EMPro system (electrodynamic analysis). When constructing the three-dimensional model of the structure under study, each element was divided into cells with the minimum size of 20 μm. An example of an RP with the same parameters is shown in Fig. 6. It can be seen that the shapes of the RP match and the maximums are close (0.0117 and 0.0068 V/m).

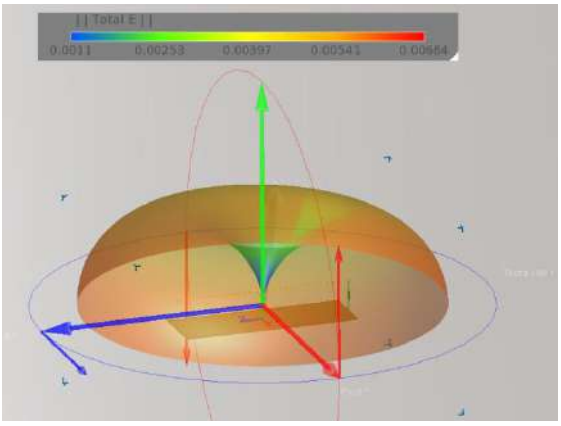

Fig. 6. An example of the RP for the ML in EMPro.

Using the temperature model from [10], we obtained the temperature dependences of the cross-section parameters and ML characteristics at the frequency of 10 GHz. The results are shown in Table 1. It can be seen that with the increase of T, the values of the parameters R and l increase, and S and $(Z_eZ_o)^{0.5}$ decrease. It is worth noting that the change in the temperature has almost no effect on the maximum value of $|E|$.

TABLE I. DEPENDENCES OF CROSS-SECTION PARAMETERS AND ML CHARACTERISTICS ON T

T, °C	R, μm	l, mm	S, μm	$(Z_eZ_o)^{0.5}$, Ohm	$\|E\|_{max}$, V/m
–50	49. 9363	29. 9617	14. 8375	136.478	0.319
–25	49. 9575	29. 9745	14. 7950	136.365	0.319
0	49. 9787	29. 9873	14. 7525	136.251	0.319
25	50	30	14.71	136.137	0.319
50	50.0212	30.0127	14.6675	136.023	0.319
75	50.0425	30.0255	14.6250	135.908	0.319
100	50.0637	30.0382	14.5825	135.794	0.320
125	50.0850	30.0510	14.5400	135.679	0.320
150	50.1063	30.0637	14.4975	135.564	0.320

The frequency dependences of the maximum value of $|E|$ (when φ and θ were changed from 0° to 180° in 1° increments) in the two systems are compared in Fig. 7.

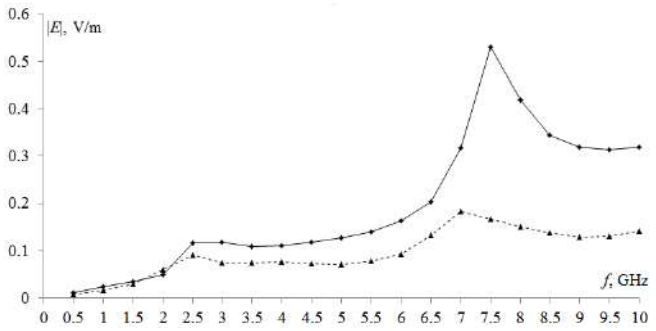

Fig. 7. The maximum frequency-dependent values of $|E|$ for the ML structure when φ and θ were chnaged from 0 to 180° in increments of 1° obtained in EMPro (- -) and in TALGAT (—) for the optimal ML parameters.

The results show that the maximum values of $|E|$ at low frequencies are close. At high frequencies, the difference between the results of quasi-static and electrodynamic analysis increases.

IV. SIMULATION RESULTS FOR UNMATCHED ML

In this section, the same structure was modeled as in Fig. 1. But, the values of $R1$ and $R2$ are assumed to be 50 Ohm. Using the models created in the previous section,

we calculated the time responses to the trapezoidal pulse (Fig. 8). It can be seen that the amplitudes of the first two pulses are uneven. The current distributions in the ML at frequencies of 0.5, 5 and 10 GHz are shown in Fig. 9. Fig. 10 illustrates an example of an RP at a frequency of 0.5 GHz and a distance of 1 m when φ and θ were changed from 0° to 180° in increments of 1° obtained in TALGAT. The maximum values of $|E|$ when φ and θ were changed from 0 to 180° in increments of 1°, depending on the frequency, are shown in Fig. 11. Moreover, similar to Fig. 7, we can notice that at high frequencies the difference between the maximum $|E|$ results of quasi-static and electrodynamic analyses increases. Fig. 12 exemplifies the comparison of the obtained results for the optimal structure and the unmatched one. As can be seen from Fig. 12, the emission from the unmatched ML is bigger due to the reflection on the ends of the ML. It is worth noting that the first occurred resonance (when the ML length $2l$ is the half of the wavelength λ=0.12 m) has the same value in the two systems but at the second one ($2l$ equal to λ/0.66 m) we can clearly notice a shift in the resonance value equal to the chosen step.

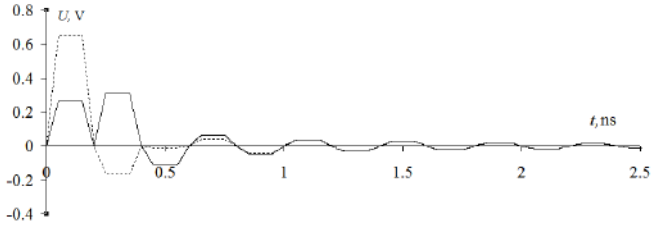

Fig. 8. The voltage waveforms at the beginning (- -) and end of the unmatched ML (—).

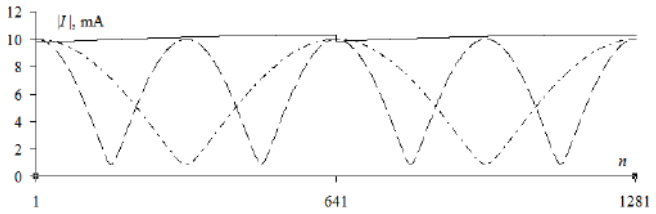

Fig. 9. The current distributions in the unmatched ML at frequencies of 0.5 (–) and 5 (- – - –) and 10 GHz (– – –).

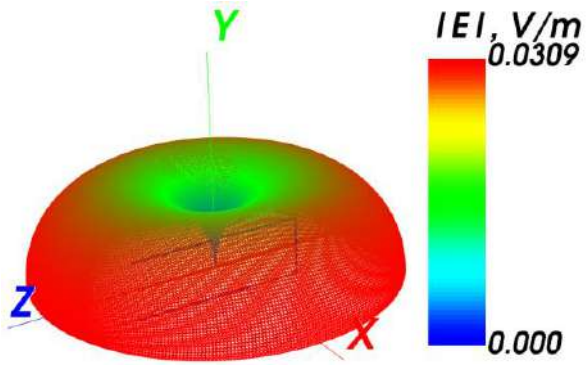

Fig. 10. An example of the RP for the unmatched ML built in TALGAT.

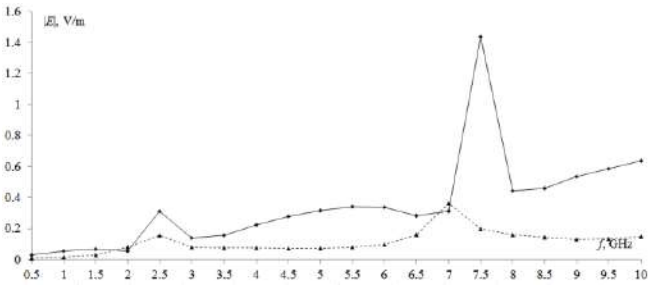

Fig. 11. The maximum frequency-dependent values of $|E|$ for the ML structure when φ and θ were changed from 0 to 180° in increments of 1° obtained in EMPro (- -) and in TALGAT (—) for the unmatched ML.

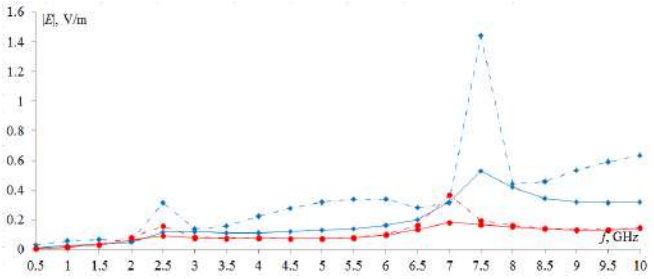

Fig. 12. The maximum frequency-dependent values of $|E|$ for a structure with an ML obtained in EMPro (–•–) and TALGAT (–♦–) for the optimal ML parameters, and in EMPro (- -•- -) and TALGAT (- -♦- -) for the non-unmatched ML.

V. COMPARISON WITH SINGLE TL

The signal in a transmission line (TL), even in a matched one where the reflection at the ends of the line is minimal, loses some of its energy emitted out from the line. Therefore, to understand the ML behavior related to radiated emission and to try to explain the signal losing its energy, we will compare the earlier results with those for one single TL imitating the expanded ML. To achieve this goal, a simple structure of a TL based on one wire above the ground plane in an air dielectric filling was modeled. The simulation was carried out without taking into account losses in the wire. The geometric model of the TL cross-section constructed in the TALGAT system is shown in Fig. 13. It has the same parameters as the ML but the length is equal to $2l$. At the near end, the line is connected to the source with the same parameters as in the ML case, and to the receiving device at the far end. Fig. 14 demonstrates the TL circuit model. The per-unit-length capacitance is taken to be equal to 10.48 pF/m calculated at the same length of subintervals.

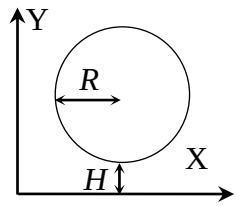

Fig. 13. The geometric model of the TL cross-section.

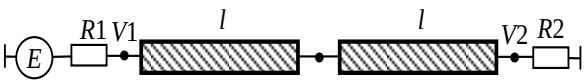

Fig. 14. The TL circuit model.

At first we consider the case of a matched TL and then an unmatched one. For the matched TL, the values of $R1$ and $R2$ are chosen to be equal to 318 Ohm, while for unmatched one equal to 50 Ohm. The voltage waveforms at the beginning and the end of the matched TL and the unmatched one are shown in Fig. 15. The amplitude of the waveform in the unmatched TL decreases, and a bigger amount of the signal energy is reflected and emitted. The current distributions were calculated and shown in Fig. 16 for the unmatched TL at the frequencies of 2.5 and 7.5 GHz. The maximum amplitude of the current in the unmatched TL increases to reach 10 mA comparing to 1.6 mA for the matched one. That will lead in general at the most frequency range to increase the maximum values of $|E|$ of the unmatched TL as seen in Fig.17. From Figs. 16 and 17 we can also notice that the signal waveforms in the unmatched TL start to take a sinusoid form because of the reflection at the ends of the TL. The RP waveforms obtained by the two systems differ a little for the unmatched TL at some frequencies, but in general we can say that the results are still acceptable. At the frequency of 2.5 GHz, an example of the RP built in TALGAT and EMPro are demonstrated in Figs. 18 and 19, respectively.

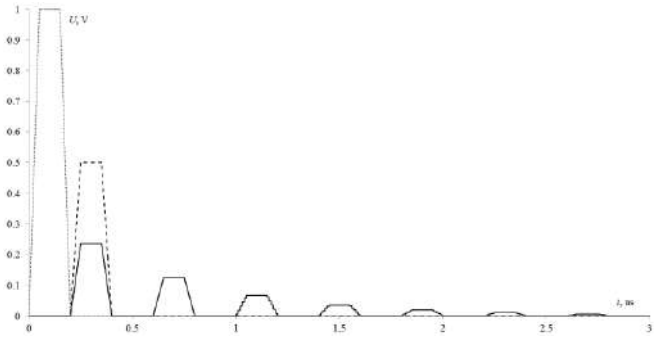

Fig. 15. The voltage waveforms at the beginning (···) and the end of the matched TL (- -) and the unmatched one (–).

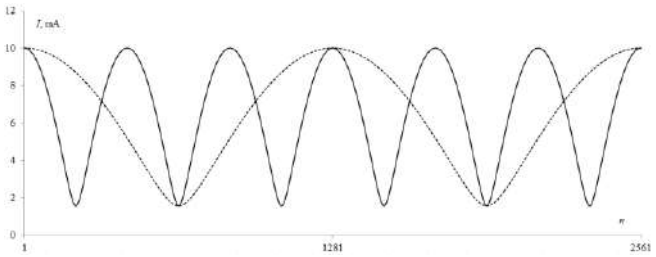

Fig. 16. The current distributions in the unmatched TL at frequencies of 2.5 (···) and 7.5 GHz (–).

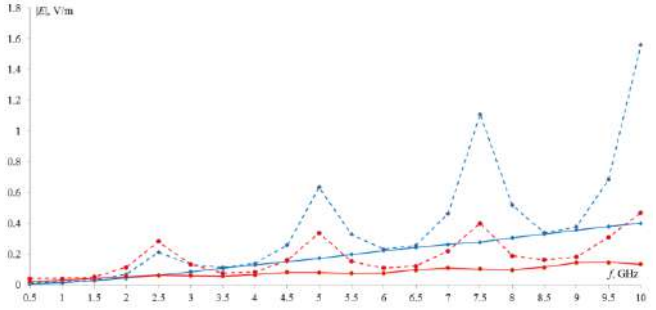

Fig. 17. The maximum frequency-dependent values of $|E|$ for the matched TL obtained in EMPro (–•–) and TALGAT (–♦–), and for the unmatched TL in EMPro (- -•- -) and TALGAT (- -♦- -).

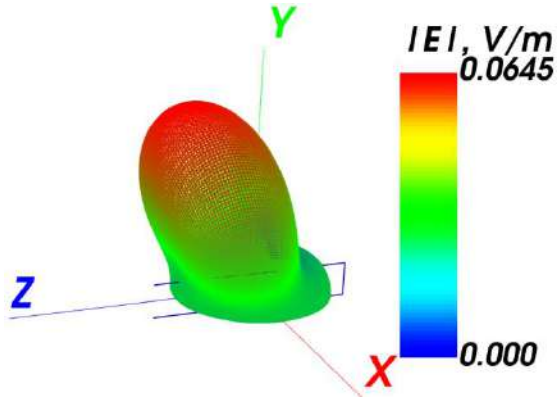

Fig. 18. An example of the RP for the TL built in TALGAT.

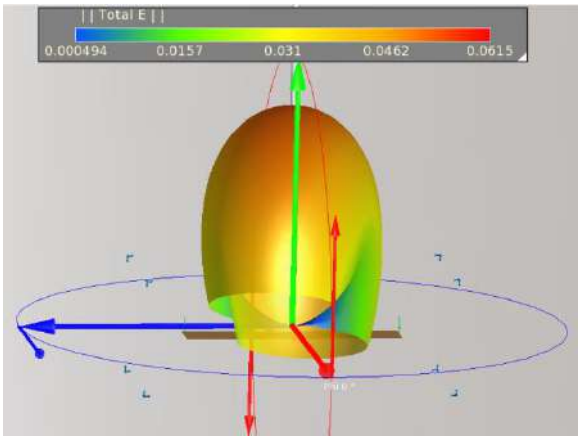

Fig. 19. An example of the RP for the TL built in EMPro.

For the matched case and the unmatched one, Figs. 20 and 21 represent comparison of the ML maximum values of $|E|$ results with TL ones, respectively. With increasing the frequency the resonance peaks become more pronounced in the matched case of ML comparing to TL. But the opposite thing is found in the unmatched case where more resonances arise at frequencies corresponding to $\lambda=2l$, l, $0.6l$, $l/2$ m. At last we can say that the ML was able to decrease the radiated emission in the most frequency range except at the resonance frequencies.

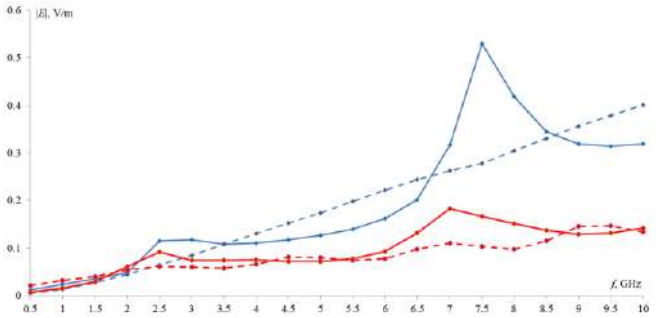

Fig. 20. The maximum frequency-dependent values of $|E|$ for the matched ML obtained in EMPro (–•–) and TALGAT (–♦–), and for the matched TL - in EMPro (- -•- -) and TALGAT (- -♦- -).

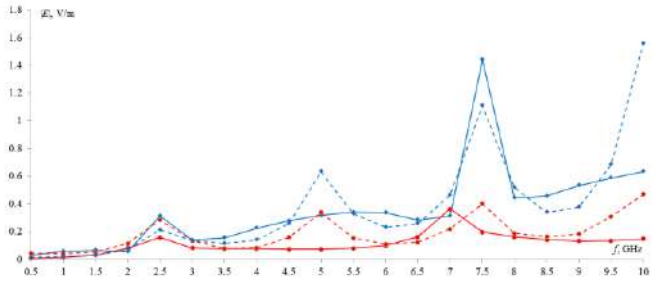

Fig. 21. The maximum frequency-dependent values of |*E*| for the unmatched ML obtained in EMPro (–•–) and TALGAT (–♦–), and for the unmatched TL - in EMPro (- -•- -) and TALGAT (- -♦- -).

It is worth noting that the proposed algorithm not only gives acceptable results comparing to electrodynamic analysis but it also remarkably decreases the computational costs. For example, simulating the unmatched single TL in the TALGAT system only took 1.48 minutes, while in EMPro system it took 30.57 minutes. This will be even bigger advantage when it comes to simulating such structures considering the losses, and this is one of the studies we are planning to do in the future.

VI. CONCLUSION

In this paper, the proposed algorithm is tested on the ML structure based on two coupled wires above the ground plane in the air. The change in temperature has almost no effect on the radiated emissions from the ML structure. The estimates of radiated emissions from the ML were obtained using two approaches. And, in contrast to the TL, the ML was able to minimize the radiated emission in the most frequency range except at the resonance frequencies. Testing the algorithm gave acceptable results at low frequencies. The results are convergent and the difference might result from using different methods; the electrodynamic analysis is based on the finite element method while the quasi-static analysis is based on the combination of the method of nodal potentials and the method of moments with thin-wire approximation (the proposed algorithm). However, obtaining closer results also depends on the chosen segmentation and getting fine-enough meshing which will be proportional to the computational cost. It is also noteworthy that the obtained results correspond to a wide frequency range but with a big step, so obviously the sampling frequency rate affects the convergence of the results. Furthermore, the results of the maximum values of |*E*|, as known, differ depending on the direction. Future work will aimed at investigating the radiated emission from this ML structure and from more complex ones taking into account the losses. In addition, a more detailed analysis should be done to achieve more close results by increasing the sampling frequency rate and running the simulation with more accurate meshing and segmentation.

REFERENCES

[1] D. A. GandolfoA. BoornardL. C. Morris “Superconductive Microwave Meander Lines,” Journal of Applied Physics, Vol. 39, pp. 2657–2660, June 1968.

[2] A. Galehdar, D. Thiel, S. G. O'Keefe, “Tapered Meander Line Antenna for Maximum Efficiency and Minimal Environmental Impact,” IEEE Antennas and Wireless Propagation Letters, Vol. 8, pp. 244–247, February 2009.

[3] L. Cheng-Ta, L. Ming-Shing, C. C.-N, “A compact dual‐band chip antenna using a nonuniform meander‐line to suppress spurious emissions,” Microwave and Optical Technology Letters, Vol. 49, pp. 773–776, April 2007.

[4] E. M. T. Jones, “Coupled-strip-transmission-line filters and directional couplers,” IRE Transactions on Microwave Theory and Techniques, vol. 4, pp. 75–81, April 1956.

[5] Y. Shlepnev, A. Neves, T. Dagostino, and S. Mcmorrow, “Measurement-assisted electromagnetic extraction of interconnect parameters on low-cost FR-4 boards for 6-20 Gb/sec applications,” Designcon, vol. 3, pp. 1290–1317, January 2009.

[6] E. Tsutomu, S. Yonehiko, S. Shinichi, K. Takashi, “Resonant frequency and radiation efficiency of meander line antenna,” Electronics and Communications in Japan (Electronics), Vol. 83, pp. 52–58, January 2000.

[7] R. Surovtsev, T. Gazizov, A. Zabolotsky, “Pulse decomposition in the turn of meander line as a new concept of protection against UWB pulses,” International Siberian Conference on Control and Communications (SIBCON), pp. 1–5, May 2015.

[8] T. Nakamura, N. Hayashi, H. Fukuda, S. Yokokawa, “Radiation from the transmission line with an acute bend,” IEEE Transactions on Electromagnetic Compatibility, Vol. 37, pp. 317–325, August 1995.

[9] A. Alhaj Hasan, A. Kvasnikov and T. Gazizov, "Approach to estimation of radiated emission from circuits with modal reservation," International Conference of Young Specialists on Micro/Nanotechnologies and Electron Devices (EDM), pp. 169–173, June 2020.

[10] I. Sagiyeva, A. Nosov, R. Surovtsev, " The influence of temperature on microstrip transmission line characteristics," International Conference of Young Specialists on Micro/Nanotechnologies and Electron Devices (EDM), pp. 191–194, June 2020.